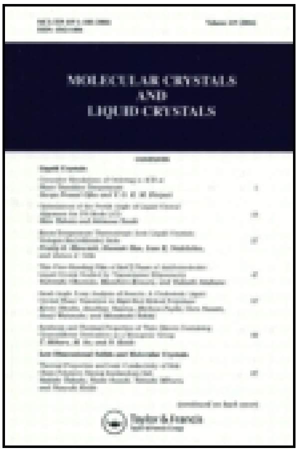

Molecular Crystals and Liquid Crystals
Publication details, including instructions for authors and subscription information:
http://www.tandfonline.com/loi/gmcl18

Structure Formation and Self-Organization Phenomena in Bistable Optical Elements

Markus Kreuzer [a] , Harald Gottschling [a] & Theo Tschudi [a]
[a] Technische Hochschule Darmstadt, Institute of Applied Physics, Hochschulstr. 6, D-6100, Darmstadt, Germany
Version of record first published: 24 Sep 2006.

To cite this article: Markus Kreuzer , Harald Gottschling & Theo Tschudi (1991): Structure Formation and Self-Organization Phenomena in Bistable Optical Elements, Molecular Crystals and Liquid Crystals, 207:1, 219-230

To link to this article: http://dx.doi.org/10.1080/10587259108032101

Mol. Cryst. Liq. Cryst., 1991, Vol. 207, pp. 219–230
Reprints available directly from the publisher
Photocopying permitted by license only

Printed in the United States of America

STRUCTURE FORMATION AND SELF-ORGANIZATION PHENOMENA IN BISTABLE OPTICAL ELEMENTS

MARKUS KREUZER, HARALD GOTTSCHLING, THEO TSCHUDI
Technische Hochschule Darmstadt, Institute of Applied Physics, D-6100 Darmstadt, Hochschulstr. 6, Germany

Abstract Transverse effects were studied in bistable optical elements with liquid crystals as nonlinear element. We present experimental results and numerical calculations on the effects of diffraction and elastic coupling on structure formation in such systems. Bistable subsystems and symmetry breaking occurs if the illuminated area is larger than the spatial resolution of the liquid crystal cell.

INTRODUCTION

Optical Bistability is well established[1] and also transverse effects in bistable optical elements have been studied for some years[2]. Investigating transverse effects and the dynamic behaviour we must distinguish between two classes of systems: (a) $\tau_{cav} > \tau_{mat}$ and (b) $\tau_{cav} < \tau_{mat}$, where τ_{cav} is the time constant of the feedback mechanism, eg. the cavity damping time, and τ_{mat} the response time of the nonlinear element. Investigations performed on the analysis of transverse effects in systems of class (a) have found e.g solitary waves[3] and spontaneous symmetry breaking[4]. Class (b) systems has been investigated only with minor influence of diffraction[5]. As recently reported[6] structure formation and symmetry breaking has been experimentally observed in *slow* systems (b) with nematic liquid crystals (NLC) as nonlinear element. The NLC shows a dispersive nonlinearity due to the reorientation of the molecules in the presence of an optical wave (electric field). To observe structure formation the spatial resolution of the NLC must be larger than the illuminated area. This spatial resolution is determined by the strong spatial coupling inside the NLC, which can be compared to the excitation of an elastic medium.

THEORY

Wave equations

In our experiment we are concerned with an nonlinear dispersive element under the influence of an external feedback mechanism. Figure 1 shows the schematic setup of an optical resonator with an intracavity nematic liquid crystal cell (NLC).

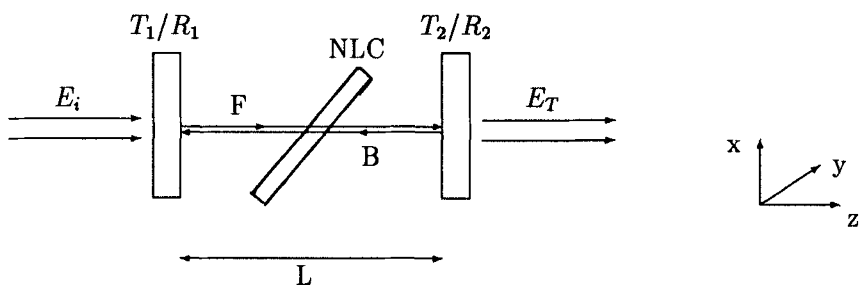

FIGURE 1 Schematic setup: L is the spacing of the two mirrors with the reflectivity R_1, R_2, resp. transmission T_1, T_2, and F/B is the forward/backward propagating field.

The incoming light is linear polarized in the (x/z)–plane. To calculate the two counterpropagating optical fields inside the cavity we use the paraxial wave equation (SVA), in which the complex amplitude of the forward and backward propagating fields (F, B) obey the form $E_{F/B} = E_{F/B}(x, y, z, t)\,\exp(\mp(i\mathbf{kr} + i\omega t)$:

$$\frac{\partial}{\partial t} F + \left(\frac{\partial}{\partial z} - \frac{i}{2}\frac{c}{\omega}\Delta_T\right) F = i\mu\omega c P \tag{1}$$

$$\frac{\partial}{\partial t} B - \left(\frac{\partial}{\partial z} + \frac{i}{2}\frac{c}{\omega}\Delta_T\right) B = i\mu\omega c P \tag{2}$$

The right hand side of Eqns. (1)(2) refers to the nonlinearity due to the optically induced reorientation $P = \varepsilon_o \chi(\theta) E_{F/B}$ (θ: angle of reorientation).

The boundary conditions are

$$E_T = \sqrt{T_2}\, F(L, t) \tag{3}$$

$$F(0, t) = \sqrt{T_1}\, E_i(t) + \sqrt{R_1\, R_2}\, \exp(i2kL')\, B(L', t - l/c) \tag{4}$$

where $\tilde{d}$ is the optical path through the NLC–cell and $l = 2(L' - \tilde{d})$ is the length of free space outside the LC. The boundary condition remains valid when we take into account the nonlinearity of the medium.

Material Equations

Using the continuum model we describe the optical nonlinearity of the liquid crystal by the macroscopic properties of the system. Assuming small reorientation angle and that the reorientation of the molecules lies in the plane of the polarization of the electric field we can write the optical energy density g_{op} and the elastic energy density g_{el} in the following form[7]:

$$g_{op} = \frac{1}{c_o}\, n_p(\theta)\, \frac{\mathbf{k}}{k}\, \mathbf{S} \tag{5}$$

$$g_{el} = \frac{K_1}{2}\left(\frac{\partial\theta}{\partial x}\right)^2 + \frac{K_2}{2}\left(\frac{\partial\theta}{\partial y}\right)^2 + \frac{K_3}{2}\left(\frac{\partial\theta}{\partial z}\right)^2 \tag{6}$$

where $\mathbf{k}$ is the wave vector, $\mathbf{S}$ is the Poynting–vector, θ is the reorientation angle, and K_1, K_2, K_3 are the Frank elastic constants while $n_p(\theta)$ denotes the effective refractive index:

$$n_p(\theta) = \sqrt{\frac{n_o^2 n_e^2}{n_e^2 \cos^2(\beta_1 + \theta) + n_o^2 \sin^2(\beta_1 + \theta)}} \tag{7}$$

Here $n_o(n_e)$ is the ordinary (extraordinary) refractive index and β_1 is the angle between the Poynting–vector and the normal of the surface of the cell inside the NLC.

Using a Lagrange formalism we get total free energy $\mathcal{F}$ of the liquid crystal, given by this two competing contributions

$$\mathcal{F} = \int_V (g_{el} - g_{op})\, dV \tag{8}$$

From previous calculations for the case of plane waves (1–dim.) we know that the reorientation angle, θ, subject to the boundary conditions

$$\theta(z=0) = \theta(z=d) = 0 \qquad (d : thickness\ of\ the\ LC - cell)$$

is a good approximation[8] by $\theta = (dz - z^2)\,\hat{\theta}(x,y)$. Here we neglect standing wave problems on the scale of λ, which will be washed out due to the strong elastic coupling inside the liquid crystal. After integrating relative to the z–coordinate we used a variational calculation with respect to $\hat{\theta}$, which gives us a Euler–Lagrange equation for the induced phase shift ϕ:

$$\tau_{LC}\,\frac{d\phi}{dt} - L_x^2\,\frac{d^2\phi}{dx^2} - L_y^2\,\frac{d^2\phi}{dy^2} + \phi = const \cdot \left(|F|^2 + |B|^2\right) \tag{9}$$

where the nonlinear phase shift ϕ, experienced by a beam in the direction s is

$$\phi = \int_0^z \vec{k}(\theta)\, d\vec{s} \tag{10}$$

In Eq. (9) we have introduced a time dependent term to describe dissipative effects due to the rotational viscosity γ of the NLC. The constants $L_x^2 = \frac{1}{10}\, d^2\, K_1/K_3$ and $L_y^2 = \frac{1}{10}\, d^2\, K_2/K_3$, which are similar to diffusion lengths, show that the spatial resolution is reduced to structures $\geq$ d. Eqns. (1)(2) and Eq. (9) form a set of nonlinear coupled differential equations. Together with the boundary conditions (eqns. (3)(4)) these are the basic equations of our model.

NUMERICAL SIMULATIONS

In our system the cavity decay time τ_{cav} and the relaxation time τ_{LC} of the NLC obey the relation $\tau_{cav} \ll \tau_{LC}$, which means that the electric field follows the nonlinearity adiabatically. In this case the the boundary conditions (3)(4) are not integrable. So we have to seperate the integration of the material equation (9) and the solution of the wave equations (1)(2). Neglecting diffraction (since $\tau_{cav} \ll \tau_{LC}$ we can make an adiabatic elimination of the electric field, taking $\partial E/\partial t = 0$) we can integrate the wave equations with respect to the boundary conditions and get

$$\tau_{LC}\frac{d\phi}{dt} - L_x^2\frac{d^2\phi}{dx^2} - L_y^2\frac{d^2\phi}{dy^2} + \phi = \frac{c_3 \cdot I_i}{1 + F\sin^2\{\frac{1}{2}(\phi_0 + \phi)\}} \tag{11}$$

The rhs of Eq. (11) shows a nonlinear Airy function, which describes the stationary state of the optical wave inside a Fabry–Perot resonator for a given phaseshift. This equation is very similar to the description of other bistable devices, such as InSb resonators, and has been investigated e.g. by Firth et. al.[5/9]

Taking diffraction problems into consideration it is not possible to find an analytic solution of the nonlinear coupled equations. To find an numerical code to solve this problems we made a seperation as mentioned above. Since the thickness $d \approx 100\mu m$ of the LC–cell is in the order of the beam waist w_o ($F = w_o^2/d\lambda \approx 10^3 \gg 1$) and $d \ll L$ we can neglect diffraction inside the LC–cell. So we determine the diffraction only by free space propagation. Changing the variables to the light frame

$$z' = z \qquad and \qquad \tau = t - \frac{z}{c}$$

we get the wave equation for the **Free Space Propagation** (FSP) ($P \equiv 0$)

$$\left\{\frac{\partial}{\partial z} - \frac{i}{2}\frac{c}{\omega}\Delta_T\right\} E = 0 \tag{12}$$

Making a Fourier transform (FT) of this equation we can integrate this equation relative to the z-coordinate. After making the inverse fourier transform (FT^{-1}) and being back in the 'lab'–system we get the complex amplitude of the electric field

$$E(z+2L,x,y) = (FT)^{-1}(\exp(\frac{i}{2}\frac{c}{\omega}(k_x^2+k_y^2)2L)\ \exp(i2kL)(FT)\,E(z,x,y) \quad (13)$$

after one roundtrip time ($\tau = 2L/c,\ z = 2L$). Equation (13) can easily be solved for an arbitary input field by using a fast Fourier transform code (FFT). This method has been investigated first by Siegmann et. al. and e.g. sucessfully used to determine mode distributions in laser systems[10].

After each roundtrip the complex input field E_i is added to the complex amplitude E. To take the Nonlinear Phaseshift ϕ (NP) into consideration the traveling waves are multiplicated with $exp(i\phi(x,y))$ in the space regime each round trip time. This procedure fulfills the boundary conditions (3)(4). The nonlinearity is held constant until getting the stationary field distribution. Then the material equation (9) is integrated for a short time $t^* \ll \tau_{LC}$ (since $\tau_{cav} \ll \tau_{LC}$) followed by FSP+NP again. So we get a temporal development of the complex amplitude of the electric field in units of t^*.

RESULTS

We set up an experiment using an plane–plane resonator with mirror (reflectivities $R_1 = R_2 = 0.9$) spacing of about $4\,cm$ and a homeotropically aligned NLC–cell ($d \approx 100\mu m$) as intracavity medium. We used a conventional liquid crystal mixture (ZLI 3219 from Fa. Merck, Darmstadt) at room temperature ($T_c = +91^oC$). The LC–cell was oriented 55^o with respect to the linear polarized laser beam.

When we drive the system with cw–Argon ion laser beam (beamdiameter $w \approx 330\mu m$, $\lambda = 514\,nm$) formation of spatial structures occurs in the transmitted light. As expected the element first shows a switching in the central part

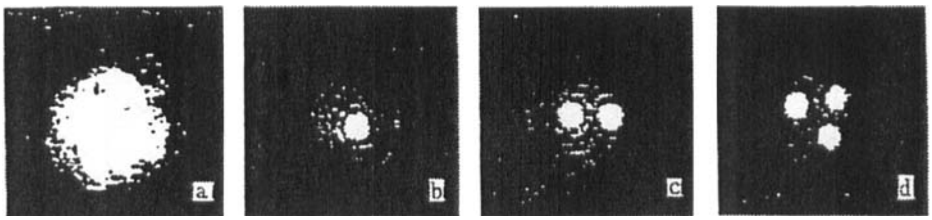

FIGURE 2 The original gaussian beam (a) and intensity distribution (b–d) in the nearfield, $w = 330\mu m$, $d = 100\mu m$.

of the beam (Fig. 2b). This onset of structure formation can be understood, if we consider the fact that the input beam has a gaussian intensity distribution. Thus by increasing the input intensity the central part of the illuminated area will switch to the 'high' state first. Then a symmetry breaking occurs and a new metastable pattern is formed. Fig. 2 shows three typical intensity distributions observed in the plane of the output mirror. In this case the distribution (d) in Fig. 2 is the stable end state. Due to the finite spatial resolution of the NLC this seems to be the best space filling pattern. An interesting fact is that these end state is very insensitive against external distortions and changes in the input intensity. Higher intensities only accelerate formation process but do not influence the form of the stable end pattern.

The formation of the structures is accompanied by a complex dynamic behaviour of the transmitted light power (Fig. 3). Decreasing the spot diameter we found a continous transition of the system to the behaviour of 'single pixel'

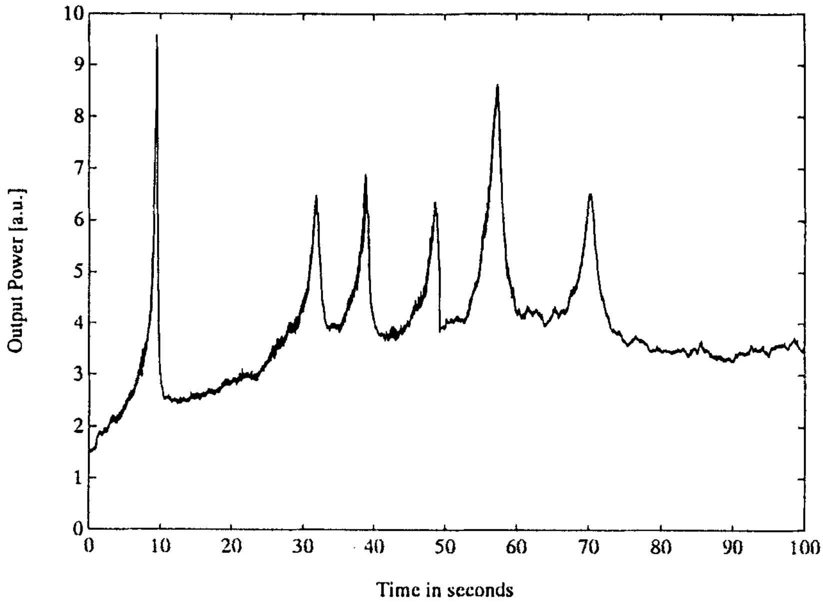

FIGURE 3 Temporal devlopment of transmitted power at constant input intensity during formation process.

bistability. While the hysteresis loop of an element with structure formation shows bistable subsystem (Fig. 4) the 'single—pixel' element shows an ideal hysteresis loop (Fig. 5). This shows that ideal bistability predicted for the case of plane waves is only a special case when the spatial resolution of the system suppresses the formation of spatial structures.

The numerical calculations have shown that symmetric solutions are very sensitive against small distortions. If we introduce a small disalignment (tilt) of about 10^{-7} to 10^{-6} rad of one of the mirrors, symmetry breaking occurs and complex structure formation appears. Nevertheless, this is still a better alignment as we can achieve in experimental work. The appearance and form of the structures are then very stable against additional distortions. This leads to the conclusion that symmetric solutions become unstable followed by a complex scenario of transitions until reaching a stable end state.

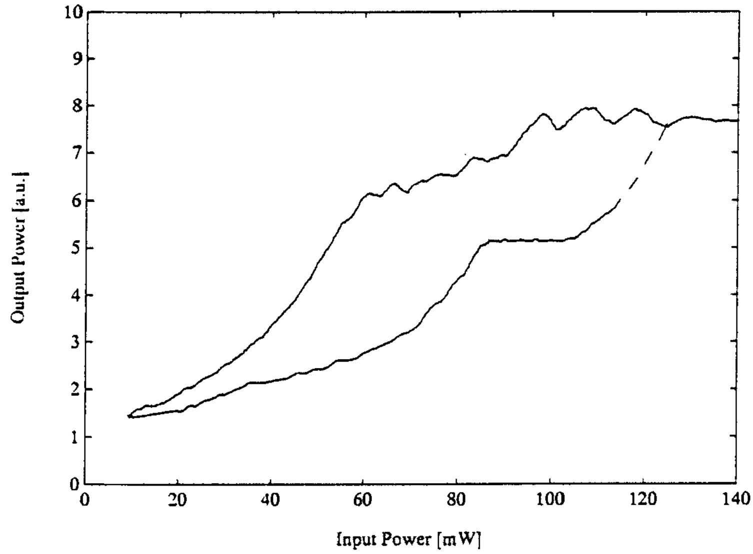

FIGURE 4 Hysteresis loop of a 'structure forming' element ($w > d$). In this loop only the stationary states (switching process at dashed line) are shown to emphasize the bistable subsystems.

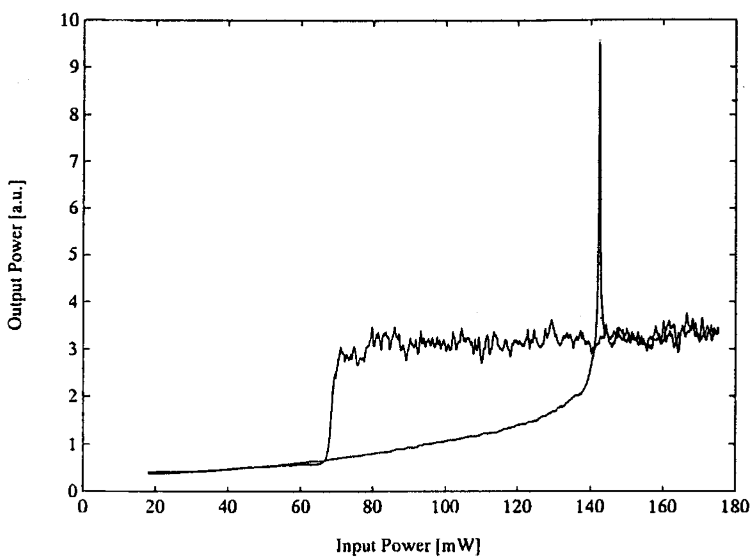

FIGURE 5 Hysteresis loop of a 'single pixel' element ($w < d$), showing ideal bistability as predicted for a 1–dimensional system.

The numerical calculation for a hysteresis loop is shown in Fig. 6, where we can see a complex switching process and the development of bistable subsystems. The intensity patterns are shown in Fig. 7. The appearance of a structure with

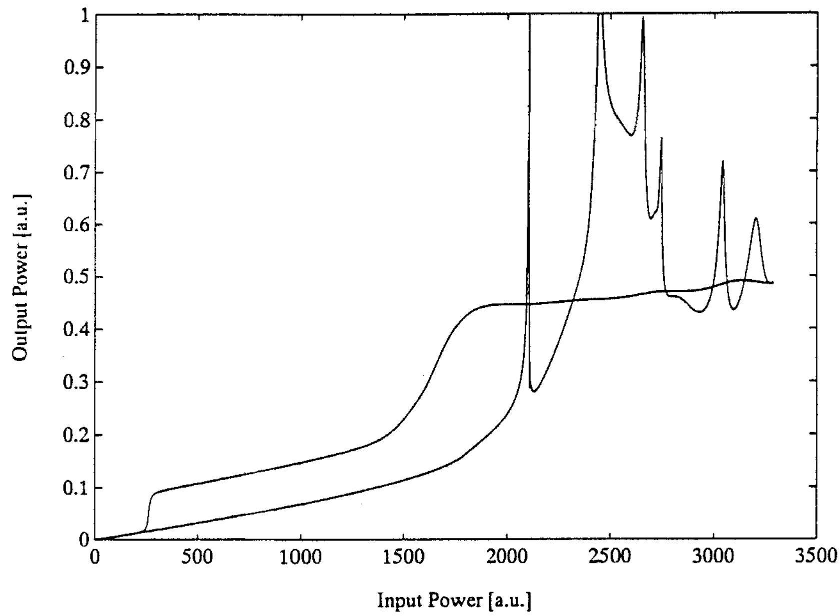

FIGURE 6 Simulation of the hysteresis loop ($w = 600\mu m$ $d = 100\mu m$) showing bistable subsystems.

'four' spots must be related to the fact that a beamdiameter of $w = 600\mu m$ was used in the numerical calculations . Now this pattern is the stable end state, which corresponds to the best space filling pattern as mentioned above.

Fig. 8 shows the numerical and experimental observation of the transition between two metastable states. It is an interesting fact that there is a short competition between the new forming peak and the old peak. The experimental results show that the transition starts at no predetermined point. So distortions, e.g. the intrinsic noise of director fluctuations, seems to play a central role by facilitating transitions between metastable patterns.

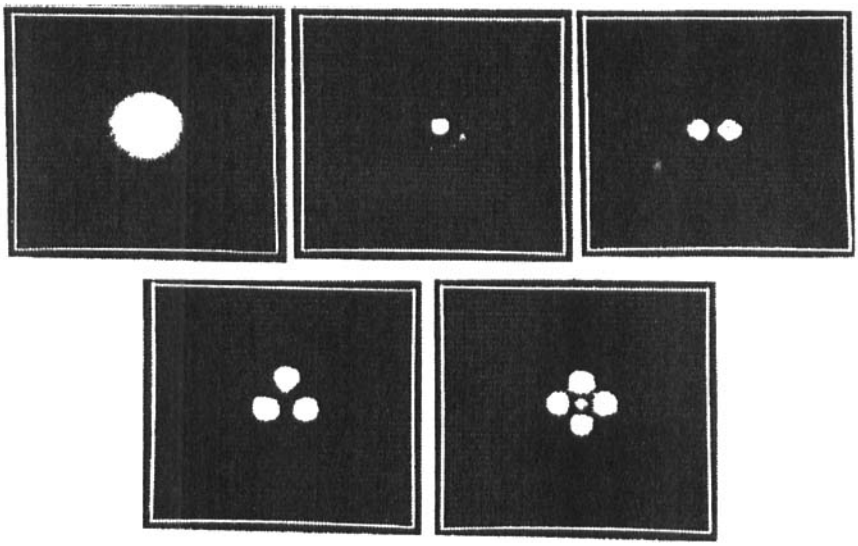

FIGURE 7 Near field structures, occured in the hysteresis loop of Fig. 6 (numerical results).

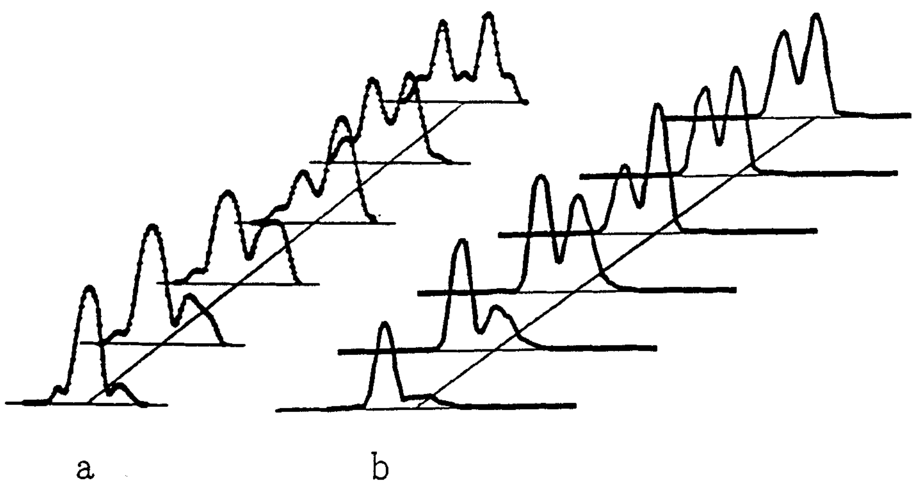

FIGURE 8 Transition from 'one spot' to 'two spots', a) experimental results, b) numerical results.

CONCLUSION

We have shown that we can achieve structure formation in optical bistable elements if the illuminated area is matched to the spatial resolution of the NLC. The dynamic processes, the 'symmetry breaking', and the fact that the stable end structure is the best space filling pattern of smallest structures, which can be resolved by the system, leads to the conclusion that this is a process of self organization. The numerical calculations shows that the wave propagation and elastic coupling have strong influence on the behaviour of the bistable element and are in good agreement with the experimental results.

ACKNOWLEDGEMENT

This work was performed within the Sonderforschungsbereich 185 Darmstadt–Frankfurt of the Deutsche Forschungsgemeinschaft. We wish to thank Fa. Merck for supporting us with liquid crystals.

REFERENCES

1. H.M. Gibbs, Optical Bistability: Controlling Light with Light (Academic Press 1985-XII).
2. J. V. Moloney, M. R. Belic, H. M. Gibbs, Opt. Commun., 41, 379 (1982).
3. H. Adachihara, D.W. Mc Laughlin, J.V. Moloney, A.C. Newell, J. Math. Phys., 1, 63 (1988).
4. A. Ouarzeddini, H. Adachihara, D.W. Mc Laughlin, J.V. Moloney, A.C. Newell, Journal de Physique, C2, C2-445 (1988).
5. W. J. Firth, I. Galbraith, J. Opt. Soc. Am. B, 2, 1006 (1985)
6. M. Kreuzer, W. Balzer, T. Tschudi, Appl. Opt., 29, 579 (1990).
7. L.M. Blinov, Electro–optical and magneto–optical properties of liquid crystals (John Wiley & Sons Ltd., Chichester 1983).
8. I.C. Khoo, J.Y. Hou, Phys. Rev. A, 27, 3251 (1983).
9. W. J. Firth, Journal de Physique, C2, C2-451 (1988).
10. E. A. Sziklas, A. E. Siegman, Appl. Opt., 14, 1874 (1975).